Fourth International Symposium on Marine Propulsors
smp'15, Austin, Texas, USA, June 2015

Systematic propeller optimization using an unsteady Boundary-Element Method

Evert-Jan Foeth
Maritime Research Institute Netherlands

Abstract
A propeller parameterization method and its application to optimize a propeller geometry in an effective wake field is presented. The parameterization is based on an analysis of over 1,250 unique propeller designs in our database and can capture most (conventional) propeller shapes. For the optimisation the genetic algorithm NSGA-II is used that quickly narrows the parameter search range.

Keywords
Propeller, parameterization, optimization

Introduction

The choice for the main propeller parameters usually follows from propeller series analysis (e.g., Wageningen B-series) and clearances to the hull based on design guidelines. Here our aim is to generate a large family of propellers and—eventually—to analyze them for their propeller-induced pressure fluctuations and efficiency; one propeller can be chosen from the results. Ideally, no rules for clearances are required. In Foeth & Lafeber [2013] a parameterized propeller geometry is described as well as the results from a calculation study using randomly generated propellers; a process that was deemed inefficient. Here we describe the procedure when we couple the propeller parameterization with a genetic algorithm called Non-Sorting Dominating Genetic Algorithm II (NSGA-II) by Deb et al. (2002). At the time being we use fully-wetted results only, or, no cavitation hindrance. However, we do include the wake field of the ship so that our exercise replaces our series analysis using only a few parameters by a propeller optimization in a wake field. The wake field follows from the optimization of the hull form of a tanker (van der Ploeg et al. 2013). So, the goal of this exercise is to minimize propulsion power by having a large population of propellers evolve without generating any geometry that is unlike a real propeller.

Propeller parameterization

The geometry of a propeller can be described in terms of radial distribution functions (ITTC Definition) or as a 3D object. The latter is often used for varying hull forms e.g., by allowing Free-Form Deformation (FFD) to obtain new hull shapes. The propeller blade is a lifting surface and the cavitation performance in the wake field is sensitive to the pressure distribution; a parameterization allows for local geometry adaptations while changing the circulation distribution but maintaining the section shape of the design and thus the lifting-surface description. The approach is reminiscent to the variation of propeller properties during manual design.

Here all geometries are analyzed using a BEM. The limitations of the BEM application with respect to the propeller geometry are documented and can be used to restrict the parameter range (e.g., restrict tip unloading); similar restrictions can follow from class strength regulations (e.g., skew angle, blade thickness); no a-posteriori analysis of the geometry is required when using parameterization to set these properties.

The propeller geometry is fully parameterized in its main parameters and its radial distribution functions for pitch, chord, camber, thickness, skew and rake. The distribution functions are replaced by rational Bezier curves consisting of no more than two line segments that are continuous in their first derivative only at their connections. Each segment is a piecewise polynomail written as a function of a parameter t as a sum of base functions β_i^n

$$c(t_j) = \frac{\sum_{i=0}^{n} \beta_i^n(t_j)\, w_i \cdot p_i}{\sum_{i=0}^{n} \beta_i^n(t_j)\, w_i} \tag{1.1}$$

with β_i^n the Bernstein polynomial in the form of

$$\beta_i^n(t_j) \equiv \binom{n}{i} t_i^i \left(1-t_j\right)^{n-i} \tag{1.2}$$

Each Bernstein polynomial runs from $t_j = 0$ to $t_{j+1} = 1$ along each curve segment defined by coordinates p_i that each have a weight w_i. Here the order n is here chosen to be $n = 3$ with four control points. The result is a cubic curve whereby p_0 and p_3 are the end points of the curve and $\overrightarrow{p_0 p_1}$ and $\overrightarrow{p_3 p_2}$ directly specify the derivate at p_0 and p_3. With these fixed end points and derivatives these curves are easy to manipulate. Some useful properties of the Bézier curves are that the curve is always boxed in within the convex hull of the points p_i (provided $w_i > 0$), the x, y coordinates of the curve depend on the respective x, y coordinates of the control points only

(i.e., no coupling between the coordinates), switching between control points and the polynomial form is straightforward and the curve can be evaluated analytically for most of its properties.

With these simple functions a series of discrete points for the radial distribution can be selected, directly linked to geometrical parameters. **Figure:** 1 shows the normalized pitch and chord distribution of a (random) stock propeller (open dots) and a best-fit of two cubic segments with uniform weights (red line); the start and end point lie at the hub and tip respectively and the center point indicates the radial position of the distribution's maximum; these are parameters that are useful to the designer.

For these two example fits, four additional points are required to determine the derivative and the curvature at the ends and center and the parameterization is mainly geared towards prescribing viable locations of these points. The center point p_3 is the maximum so p_2 and p_4 lie also at $y=1$ so that the curve remains continuous. For the chord distribution the derivative at the tip is set at $dc/dx=-\infty$ by setting $x=1$ for both p_5 and p_6. In order to reduce the number of parameters further, we set $p_1=p_2$ and $p_4=p_5$, so they lie on the intersection of the tangents to the ends of the curves and the distances to the center point p_3 are now a variable.

In order to estimate and further reduce these degrees of freedoms (or DOFs) for the chord and pitch distributions—as well as all the other functions—we have analyzed the database of propellers at MARIN containing over 1,250 unique propeller designs. A curve-fitting algorithm approximated all the radial distribution functions and returned the goodness of fit, derivative, curvature information, as well as statistical data of the parameter distributions For example, **Figure:** 2 shows the cumulative probability distribution (CDF) of the blade area ratio for fixed-pitch propellers, showing both data and an approximating function.

For most curves we estimate the derivate at p_0 and p_6 based on their relative position to p_3: if θ_1 and Θ_1 are the angles of the vectors $\overrightarrow{p_0p_3}$ and $\overrightarrow{p_0p_{1,2}}$ with the horizontal, respectively, then

$$\Theta_1=\theta_1 f\left(\theta_1,c_1\right) \tag{1.3}$$

with c_1 some constant. In **Figure: 3** the relation between θ_1 and Θ_1 for the chord distribution is presented showing the results from the database analysis and a fitting function f for several values of c_1, chosen such that the chord distribution remains monotone per piecewise element. Note that the goal is not to capture *all* points from the database but merely to capture *most* of them.

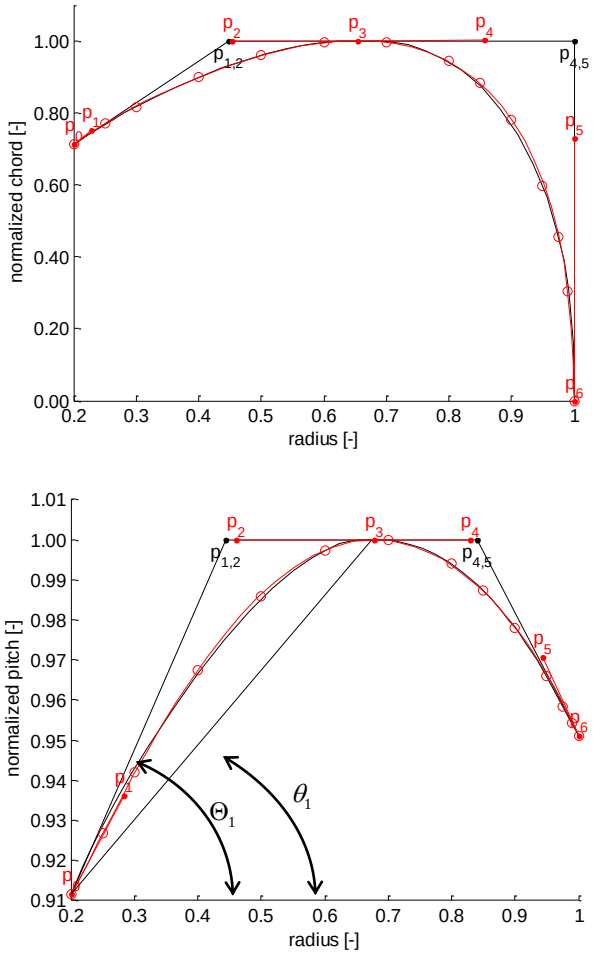

Figure: 1 Chord (top) and pitch distribution of the stock propeller showing tabular input (○), and best fits of Beziér curves (red) and the parameterization (black), including the control points of both fits. Both fits share p_0, p_3, p_7. For the parameterization points $p_1=p_2$ and $p_4=p_5$.

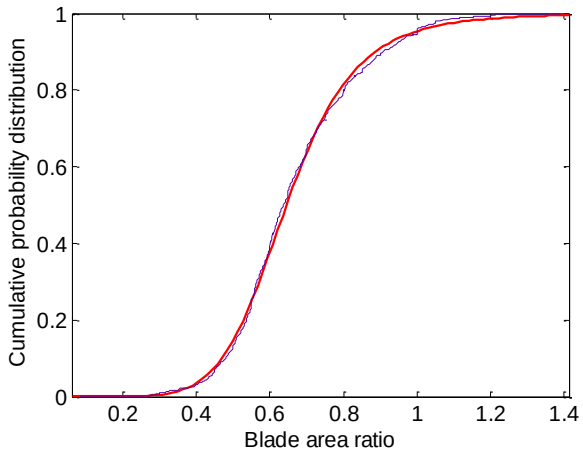

Figure: 2 CDF of the blade area ratio for fixed-pitch propellers in the MARIN database.

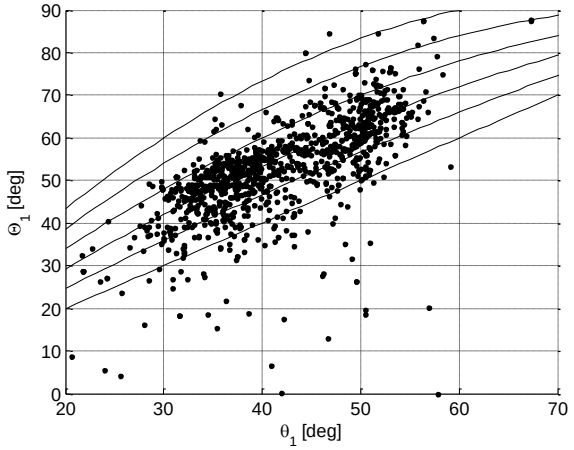

Figure: 3 Example of a database fit function, here for the derivative of the chord distribution as defined in **Figure:** 1

With each curve exceptions are encountered. For instance, for the chord distribution we demand a derivative of $dc/dr = -\infty$ at the tip so $p_{4,5}$ must lie at $[x, y] = [1,1]$ and cannot be a variable. Instead we vary the chord at the tip by modifying the weights $w_{4,5}$.

The best fit of this parameterization with the input data is also presented in **Figure:** 1 (black)—showing the coinciding points $p_1 = p_2$ and $p_4 = p_5$—demonstrating that the input data of this stock propeller can be captured by the parameterized chord and pitch functions with no more than five parameters each. Naturally, not all radial distributions of the 1,250 propellers allowed themselves to be captured this easily, but most propellers have simple distributions.

The skew of the propeller is described by a single curve segment with a given skew angle, skew bisector angle (mean skew angle) and the derivatives at the end. The camber distribution for the propellers in the database showed that over a third of all propellers have a (near) constant camber-to-chord ratio f/c but that other distributions could show much variation with resulting poorer fits using simple curves. It was observed that the oldest propellers have a constant f/c, often with sections consisting of a flat face with leading and trailing edge offsets, instead of sections using a NACA thickness/camber distribution. Here the camber-to-chord distribution was taken as a linear function with a free slope and mean. The thickness of the propeller was taken as a constant distribution. Although cavitation and weight constraints are key design issues, the thickness does not significantly influence the results from the BEM analysis for fully wetted flow.

The parameters were initially determined from the database probability functions within a preset search range given in Table 1 and were subsequently allowed to be manipulated by the optimizer within their predetermined bounds. We express the values at the hub and tip as a reduction from the maximum (unity).

The propeller analysis tool used was PROCAL, a Boundary-Element Method (BEM) developed within MARIN's Cooperative Research Ships, CRS (Bosschers et al. 2008).

Table 1 Parameter ranges

Parameter	Range
Number of blades	4
Diameter	3500-4076 mm
Blade Area Ratio	0.50 – 0.80
Chord reduction hub	0.00 – 0.70
Radial position max. chord	0.30 – 0.80
Chord reduction tip	1.00
Pitch reduction hub	0.30 – 0.80
Radial position max. pitch	0.40 – 0.80
Pitch reduction tip	0.00 – 0.40
Rake angle	-10 – 10°
Skew angle range	2 – 25°
Mean skew angle	-5 – 17.5°
Camber to chord ratio	0.00 – 0.06
Section thickness	Naca66tmb
Section camber	Naca0.8mod

Optimization routine

Generally speaking, propellers that deviate from the predetermined shaft-rate-of-revolutions show an illusory efficiency increase; it is a trivial solution to fit a ship with a propeller with a higher pitch working at a lower rpm and thus attain a higher efficiency. In order to avoid a bias to overpitched propellers, all designs were (iteratively) corrected until the design thrust was obtained within 0.1% accuracy at the design rpm; an automatic pitch correction routine steered each design towards the design point typically obtaining converge in two or three steps.

The genetic algorithm (GA) works along the principle of natural selection based on a series of optimization goals (evolutionary pressure) and population variation through cross-over and mutation of (genetic) information. Each individual is given a 'fitness value' ; fitter individuals have a better chance of staying in the population (i.e., alive) and sharing its information with other fit members to procreate a new parameter set: offspring. Here the so-called Non-dominating Sorting Genetic Algorithm II (NSGA-II) by Deb et al. [2002] was used. NSGA2 is a

generational GA; an entirely new generation is generated at each iteration instant. A *steady-state* GA will replace individual members immediately once a superior solution is found.

All results of a population are distributed in Pareto fronts that connect solutions that outperform each other on an equal number of goals and are equally 'fit'. During the evolution the number of Pareto fronts reduces and after many iterations the entire population should ideally lie on a single Pareto front: the relation between mutually exclusive optimization goals should become readily apparent and no solution is dominated by another. When solutions on the same Pareto front clutter around the same goals the NSGA-II assumes that these solutions may consist of parameters that are close and might introduce a bias towards these results. A crowding algorithm further refines the fitness by preferring solutions that are farther away from clusters of solutions and thereby maintaining genetic spread; solutions on the far edges are always considered 'non-crowded'. However, individuals that have totally different genetics but identical goal values and are hence 'diverse' could thus be penalized in their fitness; the crowding distance criterion requires further study.

A number of violations can also be included whereby the fitness of a solution degrades rapidly with an increase in the number of violations. These violations are here typically based on numerical results (e.g., poor convergence of the solution) as geometrical violations are already prevented from occurring by the settings of the parameterization. After all solutions have been ranked, the best individuals are kept for 'breeding'. This breeding process starts with a 'tournament': pairs of solutions are randomly taken and the fittest individual per paring is retained (when members are equally fit a random propeller is taken). By pairing random solutions, lesser individuals have some probability to keep sharing genetic information though the chances of these solutions on their offspring to remain within the selection of propellers decreases with each iteration.

Once this first selection is performed, the entire batch of propellers is pair-wise subjected to a 'crossover' whereby each parameter has a chance to be modified and/or exchanged between pairs. After the crossover all parameters of each new propeller have a chance to be changed randomly in the 'mutation' process. The result is the 'offspring'. Both procedures are implemented as described in Deb & Agrawal [1995]. The entire procedure is repeated several times (here 20). After a number of iterations the most dominant solutions typically transfer their properties to the population and then the only variation left is mutation. This mutation performs little better than a random search and large improvements are unexpected.

Results

In the presented analysis the focus was on an optimum in-behind efficiency, η_B. Cavitation was not included at this stage as these calculations are comparatively CPU-intensive and it is hypothesized that a first optimization is required determining the main parameter range before continuing to minimize the cavitation itself. A second substitute optimization goal was the minimization of the amplitude of the first harmonic of the propeller thrust—ΔK_T— as an indicator to far-field radiated noise to ensure interaction with the wake field (**Figure: 4**). The progression of goals as a function of the generation of 128 propellers is shown in **Figure: 5**. From the zeroth generation onward the (maximum) behind efficiency is not observed to increase much, in contrast to the decrease in ΔK_T.

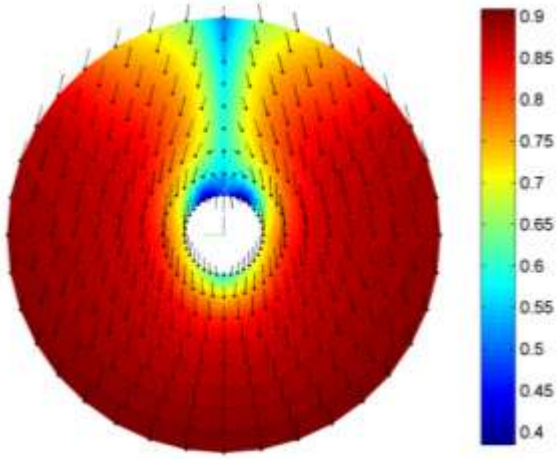

Figure: 4 Wake field, outer diameter 4067, max. tangential velocity 0.20

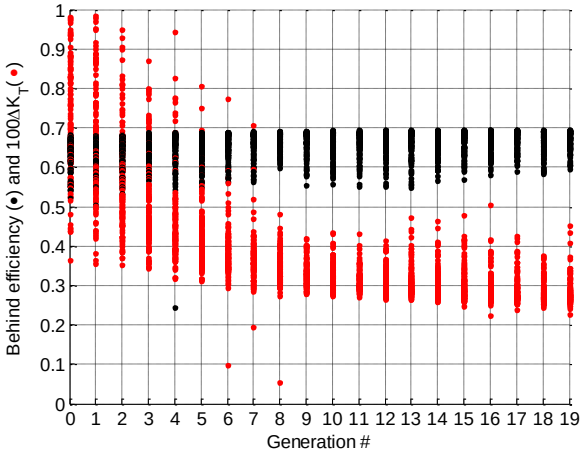

Figure: 5 Progression of evaluation goals during an optimization for the first 20 generations.

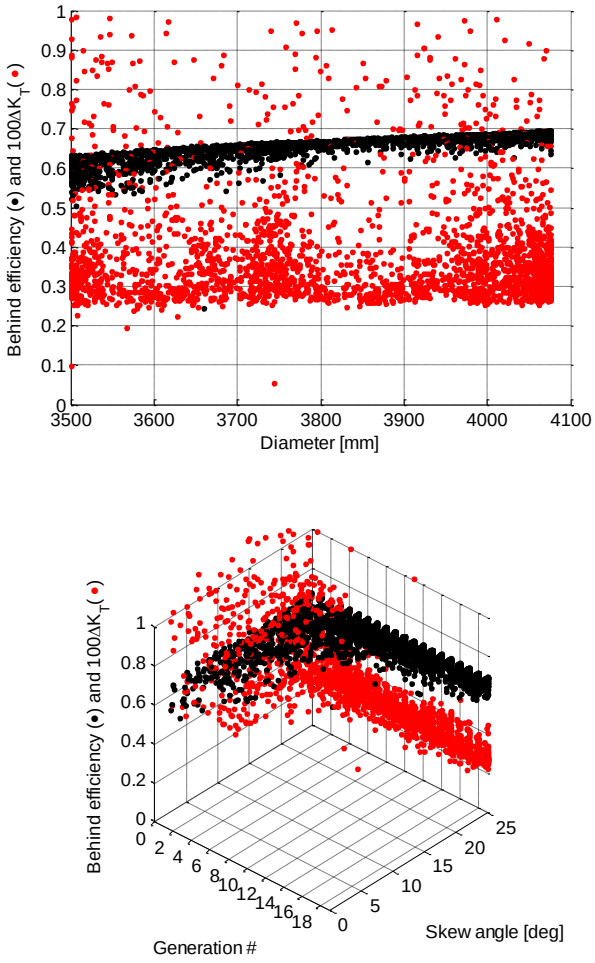

Figure: 6 Evolution of goals as a function of diameter (top) and skew angle (bottom)

When we plot the goals as a function of diameter and skew angle in **Figure:** 6 we note a clear relation of η_B with the diameter (top) and of ΔK_T with the skew angle (bottom). The GA also favors a low blade-area ratio of 0.5. Both results are not entirely trivial; a low blade area ratio leads to lower chords and thus higher reduced frequencies as the propeller blade rotates through the ship wake peak leading to an increase in ΔK_T; in addition, a smaller diameter avoids the propeller tip going through the wake peak. Here the GA avoids a high ΔK_T by selecting the maximum allowed skew angle. Although the optimum diameter of a propeller is known to be often smaller in an effective wake field, here the diameter limit (the propeller tip cannot extend below the ship baseline) determines the maximum. The optimization is repeated whereby the skew angle and diameter are fixed at their upper limits and the blade area ratio at 0.55.

In **Figure:** 7 the goal values of all solutions are shown forming a clear Pareto front[1]. The zeroeth (random) generation and last generation are highlighted. Although none of the individuals from the initial generation lie on the front—usually extinct after 3 or 4 generations—not all individuals are far removed from the Pareto front. Conversely, even though the front consists of individuals of only the last five generations, the last generation has many individuals some distance away from the Pareto front. In, **Figure:** 8, the evolution of the camber to chord ratio (f/c) at the hub and tips is shown. At the tip, f/c gravitates towards $f/c = 0.015$, while for the hub the solutions bifurcate at $f/c = 0.04$ and $f/c = 0.06$; it is occasionally observed that one bifurcation trail becomes extinct after a number of generations, which may be the case here but the number of generations is simply insufficient. The correlation between the main parameters and optimization goals of the last generation is given in Table 2 where the correlation between f/c at the hub is negatively correlated with the efficiency and the f/c at the tip is positively correlated with the thrust variations (as ΔK_T is minimized, the camber of at the tip should remain small). It is noted that most parameters do not correlate with the behind efficiency other than the a weak correlation with the camber at the hub. In order to reduce ΔK_T, from the correlation table it follows that a tip pitch reduction and a low radial position of the maximum chord are required. Counter intuitively, the value of the pitch at the tip does not correlate with at η_B all. After 20 generations the blade outline of all propellers greatly resemble the propeller in **Figure:** 9.

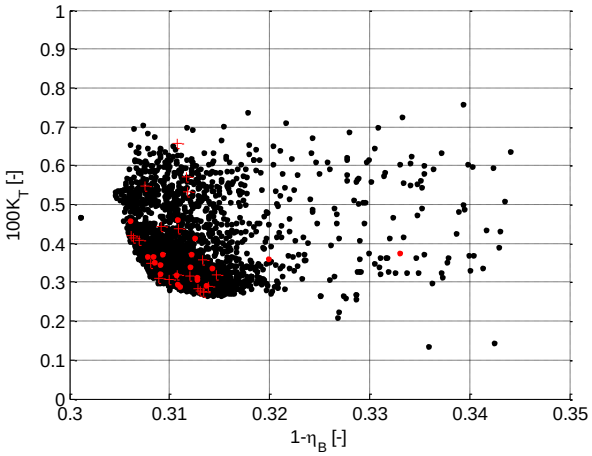

Figure: 7 All results from the 2nd alalysis showing the formation of a parameter front showing the first (•) and last (+) generations.

[1] and one exception to the left of the front that was later attributed to a meshing error; GAs

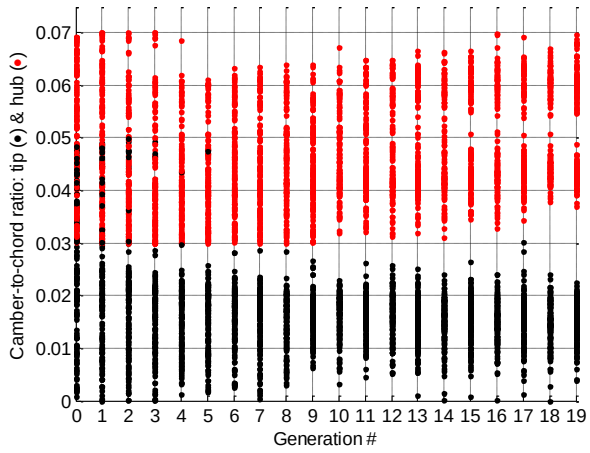

Figure: 8 Evolution of the camber-to-chord ratio

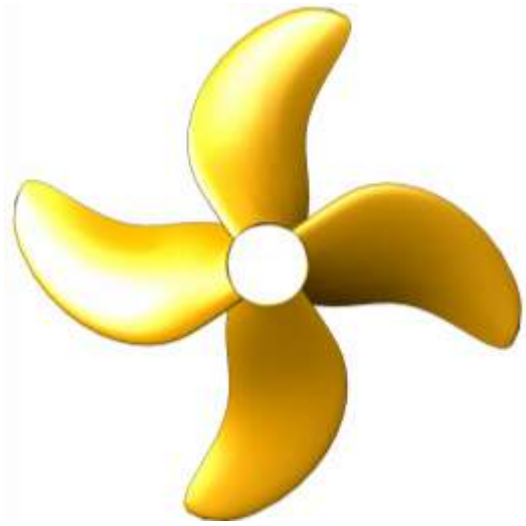

Figure: 9 Typical blade outline after 20 generations

Conclusions and discussion

A parametric propeller coupled to the genetic algorithm NSGA-2 was described and the results for a propeller optimization in a ship wake field was presented. The current method is an alternative for the determination of the main propeller parameters to the use of propeller series analysis, with the advantage of taking the wake field into account when determining the optimum diameter and giving an early advice on the camber-to-chord ratio and skew angle. From these results the search parameter range can be further reduced when optimizing for cavitation, that is, minimizing for propeller-induced force fluctuations on the hull. The next step towards fully automated propeller design is the optimization of a propeller in two wake fields simultaneously while minimizing for cavitation volume variations.

REFERENCES

Bosschers J., Vaz, G., Starke A.R., & Wijngaarden E. van, (2008). Computational analysis of propeller sheet cavitation and propeller-ship interaction, RINA CFD Marine CFD, 2008, Southampton, UK.

Deb, K., Pratap, A., Agarwal, S., & Meyarivan, T. (2002). A fast and elitist multiobjective genetic algorithm NSGA-II. IEEE Trans. on Evolutionary Comp. Vol 6(2), April 2002

Deb, K. & Agrawal, R.B. (1995). Simulated binary crossover for continuous search space. Complex systems 9, pp 115-148

Foeth, E.J. & Lafeber, F.H., (2013). Systematic propeller optimization using an unsteady Boundary-Element Method. 12th Int. Symp on Practical Design of Ships and Other Floating Structures 20-25 October 2013, Changwon, South Korea.

van der Ploeg, A. & Foeth, E.J. (2013). Optimization of a chemical tanker and propeller with CFD. 5th int. conf. on comp. meth. marine eng., 2013, Hamburg, Germany

Table 2 Correlation between the various propeller parameters and optimization goals

	Chord reduction hub	Rad. pos. max. chord	Chord reduction tip	Pitch reduction hub	Rad. pos. max. pitch	Pitch reduction tip	f/c hub	f/c tip	Rake	Behind efficiency	Thrust Variations
Chord reduction hub	1.00	-0.07	0.05	0.15	-0.13	0.05	0.12	-0.04	0.02	-0.11	-0.09
Rad. pos. max. chord	-0.07	1.00	-0.01	0.10	0.03	-0.19	-0.06	0.10	0.09	-0.16	0.37
Chord reduction tip	0.05	-0.01	1.00	0.00	0.02	0.09	0.07	-0.05	0.11	-0.17	0.02
Pitch reduction hub	0.15	0.10	0.00	1.00	0.13	-0.05	-0.24	0.11	0.17	0.14	0.05
Rad. pos. max. pitch	-0.13	0.03	0.02	0.13	1.00	0.10	-0.04	-0.05	-0.09	0.10	-0.18
Pitch reduction tip	0.05	-0.19	0.09	-0.05	0.10	1.00	0.15	-0.26	-0.25	-0.01	-0.36
f/c hub	0.12	-0.06	0.07	-0.24	-0.04	0.15	1.00	-0.18	-0.31	-0.28	-0.16
f/c tip	-0.04	0.10	-0.05	0.11	-0.05	-0.26	-0.18	1.00	0.29	0.20	0.57
Rake	0.02	0.09	0.11	0.17	-0.09	-0.25	-0.31	0.29	1.00	0.01	0.79
Behind efficiency	-0.11	-0.16	-0.17	0.14	0.10	-0.01	-0.28	0.20	0.01	1.00	0.02
Thrust Variations	-0.09	0.37	0.02	0.05	-0.18	-0.36	-0.16	0.57	0.79	0.02	1.00